Theoret. chim. Acta (Berl.) 24, 346—370 (1972)

Porphyrins XXIV. Energy, Oscillator Strength, and Zeeman Splitting Calculations (SCMO-CI) for Phthalocyanine, Porphyrins, and Related Ring Systems

A. J. McHugh* and Martin Gouterman
Department of Chemistry, University of Washington, Seattle, Washington 98105

Charles Weiss, Jr.*
Lawrence Radiation Laboratory, University of California, Berkeley, California 94720

Received May 17, 1971

Extensive CI calculations have been done on free base porphin and the metallo derivative of porphin, tetrazaporphin, phthalocyanine, various benzporphins, chlorin, and bacteriochlorin. The transition gradient operator gives good agreement with experimental intensities. Free base porphin may have a weak $\pi - \pi^*$ transition around 480 *nm*. Tetrabenzporphin and phthalocyanine are predicted to have much more intensity around 50000 cm^{-1} than porphin and tetrazaporphin due to benzenoid transitions, a prediction borne out by the available data. Magnetic effects are calculated for the low energy excited states. Q state angular momentum is calculated to be 4.35 $\hbar$ for porphin and 3.13 $\hbar$ for phthalocyanine. Although these numbers agree with some experimental results, the calculations show that the experimental analysis needs further refinement.

Es wurden ausführliche CI-Rechnungen für die freie Porphinbase und die Metallderivate von Porphin, Tetrazaporphin, Phthalocyanin, verschiedene Benzporphine, Chlorin und Bacteriochlorin durchgeführt. Der Operator des Übergangsgradienten zeigt gute Übereinstimmung mit experimentellen Intensitäten. Die freie Base Porphin hat höchstwahrscheinlich bei 480 *nm* einen schwachen $\pi - \pi^*$-Übergang. Mit Hilfe der vorhandenen Daten ist die Voraussage möglich, daß die benzoloiden Banden im Bereich um 50000 cm^{-1} im Falle von Tetrabenzporphin und Phthalocyanin intensiver als bei Porphin und Tetrazaporphin sind. Ferner werden die magnetischen Eigenschaften für angeregte Zustände niedriger Energie berechnet. Man erhält den Drehimpuls des Q-Zustandes zu 4,35 $\hbar$ für Porphin und 3,13 $\hbar$ für Phthalocyanin. Obwohl diese Werte mit einigen experimentellen Resultaten übereinstimmen, zeigen die Rechnungen, daß die experimentelle Analyse weiterer Verfeinerung bedarf.

1. Introduction

Gouterman and Wagnière [1] showed that the four orbital model could explain many of the observed features of porphyrin spectra. The model is based on the assumption that transitions between the two top filled orbitals and the two lowest empty are relatively well separated from the remainder. SCMO–PPP–CI calculations (self-consistent molecular orbital-Pariser-Parr-Pople-configuration interaction) performed by Weiss, Kobayashi, and Gouterman [2] showed that the four orbital model was justified for the lowest energy transitions (Q bands) but was less justified for the near *uv* (Soret or B) transitions. These better calculations predicted various higher transitions; the main weakness was the overestimation of the $Q - B$ splitting and the gross overestimation of oscillator strength.

* Present address: See end of paper.

This paper extends the previous SCMO–PPP–CI study in the following ways: For porphin and tetrazaporphin (TAP), for which full CI has been reported, we have used the transition gradient operator [3] for the calculation of oscillator strength, obtaining good agreement with experiment. We also report a full CI treatment of phthalocyanine (Pc) and tetrabenzporphin (TBP), which were previously done only with the four-orbital model, and the mono, di, and tribenzporphins, which were previously not studied. Section 2 reports the results for the energy and oscillator strength calculations. Section 3 uses these wave functions to calculate Zeeman splitting integrals previously only reported within the four-orbital model [4]. For these latter calculations chlorin and bacteriochlorin are included.

2. SCMO–PPP–CI Energies and Oscillator Strengths

a) Method

The SCMO–PPP method was used to generate a basis for an extensive singly excited CI treatment. The choice of configurations was based on energetic considerations and was limited by the available core storage space in the 7094 computer. General policy was to include all configurations up to 66666 cm^{-1}, but for the larger molecules this was not practicable.

The choice of semiempirical parameters followed the "traditional" set espoused by Weiss *et al.* [2], mostly for consistency but also in the knowledge that this set has already given a good account of itself in previous calculations. The parameters are:

$$\begin{aligned} (ii|ii)_C &= 10.60\,\text{eV}, \qquad (ii|ii)_N = 13.31\,\text{eV}, \\ W_C &= -11.22\,\text{eV}, \qquad W_N = (-36.61 + 11.05p)\,\text{eV} \end{aligned} \tag{1}$$

where $p = 1$ for pyrrole, 1.5 for neutral porphyrin, and 2 for pyridine. The 1.5 value was used for the central N atoms except for the free base porphin calculation. The Mataga and Nishimoto [2, 5] formula for the Coulomb repulsion integrals γ_{ij} was used and the resonance integrals were given by

$$\beta_{ij} = \frac{-2.371\,S(R_{ij})}{S(1.39\,\text{Å})}\,\text{eV} \tag{2}$$

where $S(R_{ij})$ is the two center overlap integral. The geometry of Hoard *et al.* [6], artificially constrained to planar square symmetry, was used for porphin, tetrazaporphin, and the benzporphins [2]. Robertson's [7] geometry was used for phthalocyanine. After the MO's were obtained, the CI matrix elements were calculated among the allowed singly excited states.

Diagonalization of the resulting matrix gave our final allowed electronic states. Forbidden states were calculated separately in order to reduce the size of the matrices generated in the CI treatment. In calculating f_1 and f_2 we made use of Eqs. (7) and (8) of Ref. [3] using theoretical values for the energies. For the D_{4h} molecules reported in Table 1 and Figs. 1, 3, 4, and 7, the theoretical f values are for one transition of a degenerate pair. The experimental f values are obtained from

$$f = 4.33 \times 10^{-9} \int \varepsilon d\tilde{\nu}.$$

Thus for the D_{4h} cases theoretical f values must be doubled when comparing with experimental f values.

Some comparison of the parameters given above with the set more carefully worked out be the Stockholm group [9a, 9b, 9c] is in order. We find two principal differences: (i) The Stockholm one center parameters W_μ are 1.4 to 2 eV less negative than the ones we use; (ii) The Stockholm one center electron repulsion integrals $(ii|ii)_\mu$ are 1.4 to 2 eV more positive. The resonance integrals β_{ij} are not so different. The Stockholm value for the lowest ionization energy for free base porphin is ~ 6.5 eV [9c], while our value is ~ 8.5 eV [2]. Since the Stockholm parameter set was developed to fit among other data the ionization potentials of a set of small molecules, their value should be more reliable. Their calculations and ours give a rather similar account of the absorption spectra. The gap between visible and Soret bands, too large for both calculations, is somewhat smaller with our parameter set. Knop and Knop [9d] used values for W_μ and $(ii|ii)_\mu$ close to the values we have used except they used $(ii|ii)_N = 16.57$ eV and $\beta_{CN} = -1.8$ eV for pyrrole nitrogen. Their resulting free base porphin spectrum is rather similar to the one reported here.

b) Free Base Porphin (P)

Table 1 and Fig. 1 give energies and oscillator strengths for all transitions out to 60000 cm^{-1}. Three calculations are reported: $\Delta\alpha = 0$, 5.5 eV, and 11.05 eV, where $\Delta\alpha = \alpha_N$ (pyridine) $- \alpha_N$ (pyrrole). The last gives normal pyridine and pyrrole coulomb integrals to the central nitrogens of the free base, while the first corresponds to the metal. Several features are notable: (i) The f_2 (gradient) value for the near uv absorption agrees with experiment while the f_1 (dipole) value is large by a factor of 4. (ii) The gradient operator, but not the dipole operator, correctly predicts Q_y to be more intense than Q_x [8]. This last result can be obtained from the dipole operator if a somewhat different Hamiltonian is used [2, 9c]. (iii) At $\Delta\alpha = 5.5$ eV the B intensity is divided between three bands B_x, B_y, N_x. At $\Delta\alpha = 11.00$ eV the B intensity is primarily in the fourth and fifth excited states with the third band moderately intense. (See Table 1 and Fig. 1.) For both $\Delta\alpha$ values there is substantial splitting among the intense components of the B region. A similar result is found by Sundbom [9c] using somewhat different parameters.

Earlier interpretation of the porphin spectrum [10] assigned as B_x and B_y the two peaks of nearly equal intensity separated by 240 cm^{-1} observed by Rimington *et al.* [8] in the low temperature absorption spectrum. However this interpretation is incompatible with the calculated results for either $\Delta\alpha = 5.5$ eV or 11 eV. As shown in Table 1, for $\Delta\alpha = 0$ corresponding to a metal porphin, there are five principal bands Q, B, N, L, M calculated for $\lambda > 200$ nm. The Q band is expected to be very weak ($f_2 = 0.001$) while the B band is strong ($f_2 = 0.57$) [N.B.: These f_2 values refer to one component of a degenerate pair of transitions.] At $\Delta\alpha = 11$ eV the B band intensity appears in two transitions at 28370 cm^{-1} and 30310 cm^{-1} and an electronic band with $f_2 = 0.07$ is predicted to be between Q and B. Actually two pieces of data confirm the spreading of B band intensity: (i) Polarization data of Sevchenko, *et al.* [11] show positive and negative polarization regions of the B band separated by 600 cm^{-1}. (ii) The vapor and solution

Table 1. Oscillator strength for excited states of porphin as a function of α values

Metal State	Energy (cm^{-1})	$\Delta\alpha = 0$[a] f_1	f_2	Energy (cm^{-1})	$\Delta\alpha = 5.5$ f_1	f_2	Energy (cm^{-1})	$\Delta\alpha = 11.05$[b] f_1	f_2
Q	15937	0.002	0.001	14989x	0.01	0.000	13553x	0.029	0.000
	x, y			16913y	0.000	0.002	17247y	0.005	0.004
B	28403	2.82	0.57	27524x	1.67	0.30	24930x	0.48	0.07
	x, y			28794y	3.06	0.67	28371y	2.73	0.58
N	33920	0.34	0.08	31667x	1.79	0.47	30307x	2.80	0.61
	x, y			35010y	0.19	0.08	32940y	0.38	0.10
L	37377	0.15	0.06	38423y	0.16	0.06	41965y	0.04	0.01
	x, y			40175x	0.11	0.06	42005x	0.12	0.06
	47563	0.02	0.001	47023x	0.11	0.05	43997x	0.34	0.14
	x, y			47599x	0.08	0.05	45358x	0.008	0.003
M	48007	0.07	0.05	47904y	0.02	0.001	46982y	0.001	0.001
	x, y			49118y	0.03	0.009	47947y	0.04	0.000
	50588	0.02	0.03	49905x	0.04	0.006	48788y	0.01	0.02
	x, y			50274y	0.001	0.006	49482x	0.02	0.03
	52208	0.07	0.01	52659x	0.000	0.008	52385x	0.03	0.03
	x, y			53539y	0.008	0.003	52808y	0.006	0.001
	53613	0.004	0.002	54513x	0.006	0.003	54214x	0.003	0.001
	x, y			56438y	0.06	0.02	56062y	0.19	0.11
	58297	0.09	0.03	59144x	0.11	0.03	57695x	0.09	0.04
	x, y			59553y	0.005	0.000	58176y	0.21	0.07
	59364	0.11	0.08	59665y	0.13	0.06	58713y	0.05	0.02

[a] Metal case; f values for one of the degenerate transitions.
[b] "Traditional" free base value.

spectra of Edwards [12] show unusual broadness of the Soret region in free base compared to metal complexes. Therefore we now assign the two peaks separated by 240 cm^{-1} observed by Rimington *et al.* [8] to a Shpol'skii or dimer splitting and believe the B intensity is spread among more widely separated electronic origins.

The facts known at present do not allow a clear choice between the $\Delta\alpha = 5.5$ eV and $\Delta\alpha = 11$ eV calculations. The vapor spectrum of Edwards [12] shows a very broad absorption between 25000 cm^{-1} and 32000 cm^{-1}, which contains the Soret intensity. A double L band ($f \sim 0.1$) is observed at 34250 and 37700 cm^{-1}. Finally an M band ($f \sim 0.3$) is observed at 44400 cm^{-1}. In addition we might note that a weak peak at $\sim$21000 cm^{-1} has been consistently observed by Longo and coworkers [13] in substituted free base tetraphenylporphins between $Q_y(1, 0)$ and the Soret band. It can also be observed in free base octaethylporphin [12a], and possibly one of the peaks in free base porphin in the region $\lambda \sim 485$ *nm* [8] is of the same origin. In the study of Longo *et al.* the intensity of this band depends on substituent, as might be expected for an electronic band. However its intensity is far less than $f_2 = 0.07$ predicted by the $\Delta\alpha = 11$ eV calculation for the band at 24930 cm^{-1} lying between the intense Soret bands and the two Q bands.

We can relate the $\Delta\alpha = 5.5$ eV calculation to the data as follows: (a) The "Longo" band at 21000 cm^{-1} is either Q (2, 0) or perhaps $n - \pi^*$; (b) the Soret intensity of Edwards is related to three intense calculated bands between 27520 cm^{-1} and 31670 cm^{-1}; (c) the L bands of Edwards are assigned to calcu-

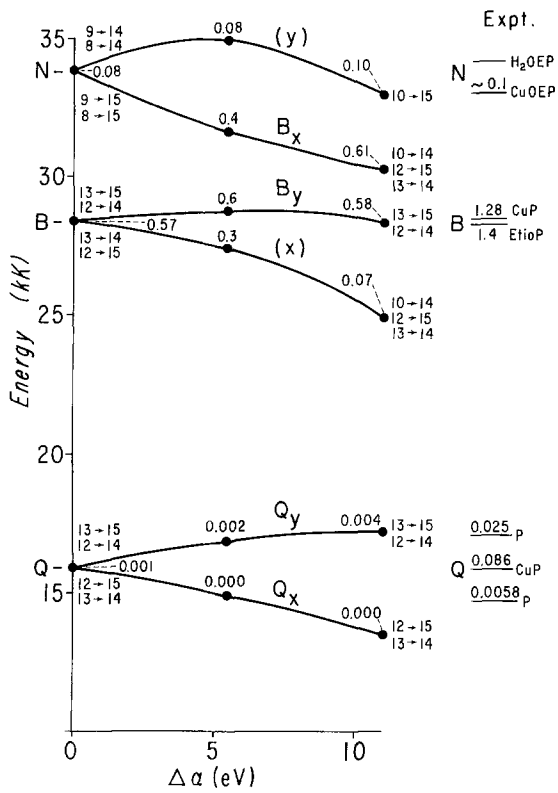

Fig. 1. Energy levels for porphin: $\Delta\alpha = 0$ corresponds to metal while $\Delta\alpha = 11.05$ eV to free base. (see Sect. 2b.) Orbitals 8, 9, 13 are b_{1u} symmetry; orbital 12 is a_u; orbital 14 is b_{2g} (nodal plane yz); orbital 15 is b_{3g} (nodal plane is xz). See Fig. 9 for axes. Theoretical f_2 values are given. Experimental values of CuP and etioporphyrin from Ref. [33]. "Longo" band (see text) at 21000 cm^{-1} not shown

lated bands at 35010 cm^{-1} ($f_2 = 0.08$) and 38420 cm^{-1} ($f_2 = 0.06$); (d) the Edwards M band is the three bands at ~47000 cm^{-1} with combined $f_2 \sim 0.1$; (e) the calculated band at 40180 cm^{-1} ($f_2 = 0.06$) is probably the M region. Sundbom [9] gave a similar interpretation for the free base porphin spectrum, placing two strong bands in the region 25000 to 31000 cm^{-1}. Her calculated $n - \pi^*$ transition is at 31600 cm^{-1}, rather to the blue of the "Longo" band.

We can relate the $\Delta\alpha = 11$ eV calculation to the data in a different way: (a) The "Longo" band is ascribed to the $\pi - \pi^*$ band ($f_2 = 0.07$) predicted to lie between the Soret and visible bands; (b) the Soret band of Edwards is related to the two intense transitions calculated for 28370 cm^{-1} and 30310 cm^{-1}; (c) the Edwards L band is ascribed to the predicted band at 32940 cm^{-1} ($f_2 = 0.10$); (d) the Edwards M band is ascribed to the calculated band at 44000 cm^{-1} ($f_2 = 0.14$); (e) the calculated band at 42000 cm^{-1} ($f_2 = 0.06$) is probably in the M region.

An interpretation generally similar to this was proposed by Knop and Knop [9d], except they identified the strongest visible band (generally called Band IV) as the electronic transition between the visible bands and the Soret. Their primary

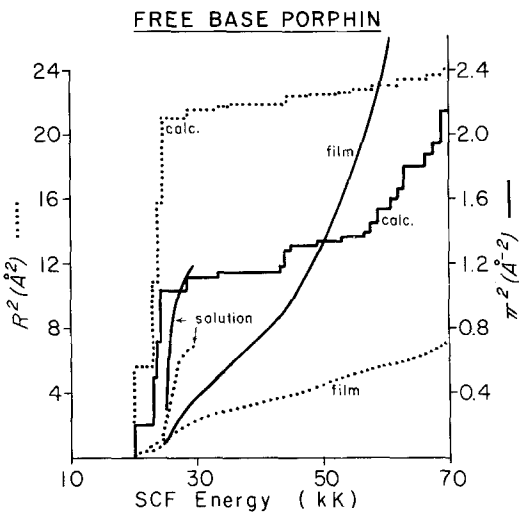

Fig. 2. Solution data [14], film data [15], and calculated values (from one-electron transitions) for R^2 (dotted lines) and Π^2 (solid lines). See Ref. [3] for detailed explanation of these plots

evidence for this was the positive fluorescence polarization. Since such polarization is predicted by vibronic considerations (see Ref. [32]), we do not find this argument compelling.

We can see that neither the calculations for $\Delta\alpha = 5.5$ eV nor those for $\Delta\alpha = 11$ eV match the vapor spectrum of free base porphin well enough for us to choose unambiguously between them. Both predict that the B intensity will be spread out and that beyond the B region there will not be much intensity. If substituent effects on intensity and polarization studies can establish that the "Longo" band at 21000 cm^{-1} represents the origin of a $\pi - \pi^*$ electronic transition, then the $\Delta\alpha = 11$ eV calculation will take precedence. As discussed below, MCD results are ambiguous on this point, and for the present the question remains unsettled.

Finally we compare the absolute value of calculated intensity to experiment in Fig. 2 using the cumulative total integrated absorption strength, a method of presentation used before [3]. The reported data come from solution data [14] and from recent data on protoporphyrin films [15]. There is considerable disagreement between these data sources, which might arise from errors in crystal thickness or density. The theoretical Π^2 value agrees well with the solution Π^2 value suggesting that Schechtman's crystal values are too low since there is considerable solution data. The calculated R^2 are much greater than experimental, as found for numerous aromatic hydrocarbons [3].

The rapid divergence between the film Π^2 and calculated Π^2 above 50000 cm^{-1} can be explained in terms of the presence of transitions to conducting states. Schechtman [15] has noted that continuum transitions appear at least as low as 30000 cm^{-1} in free base porphin. Conducting states are necessarily collective in nature and are outside the scope of the present isolated molecule calculations.

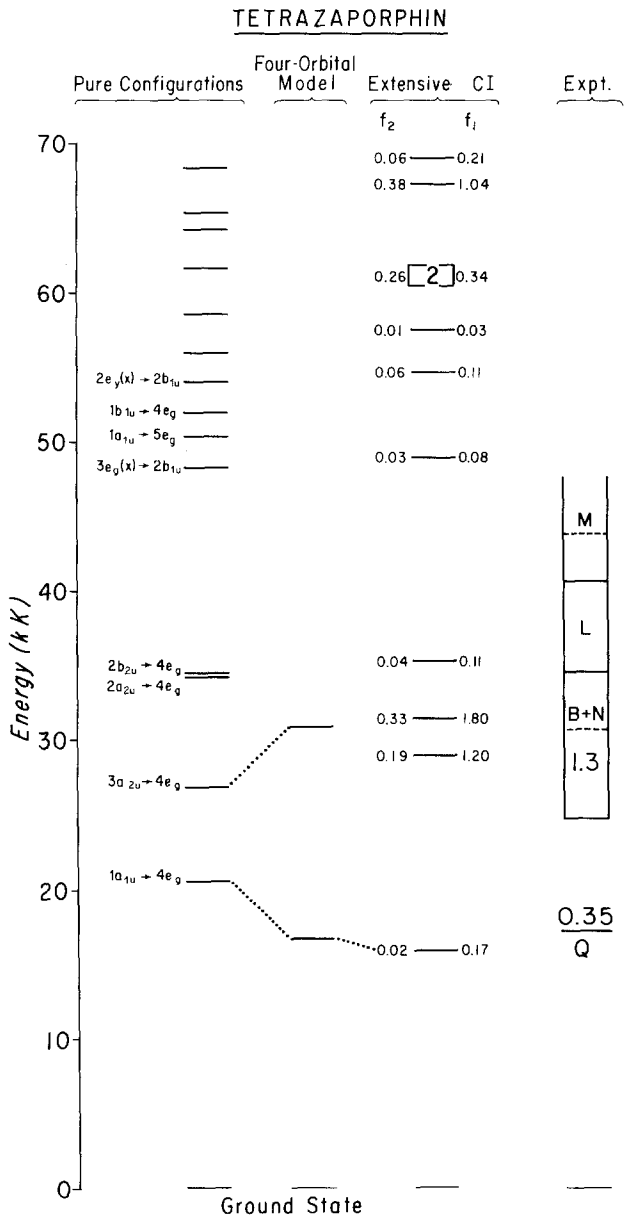

Fig. 3. Allowed transitions with and without CI with theoretical f_1 and f_2 values. Transitions with f_1 and f_2 below 0.01 are deleted. Integers in theoretical boxes give number of predicted levels. Experimental data from Linstead [private communication] on MgTAP in methanol. Continuous absorption above 24.6 kK indicated by box: solid lines show minima and dashed lines peaks. Numbers give experimental f values

c) Tetrazaporphin

The present SCMO–CI calculation employed a slightly higher cut-off energy than that of Weiss *et al.* [2], but the energy level diagram in Fig. 3 is very similar. Both transition gradient and dipole calculations predict a stronger N than B band. We believe the data supports this interpretation [14b], although our interpretation has been criticized (Ref. [11b], p. 167). The diffuseness of the composite B, N bands might be attributed to a strong vibronic interaction between the two. However, Hochstrasser and Marzzacco [16] have pointed out that interaction between $n-\pi^*$ and $\pi-\pi^*$ transitions is more effective in causing diffuseness than interaction between two $\pi-\pi^*$ transitions. Recent extended Hückel calculations on tetrazaporphin indicate the presence of $n-\pi^*$ transitions in the B, N region [17]. In view of the fact that the diffuseness of the B, N region in tetrazaporphin and phthalocyanine greatly exceeds that in the comparable region of porphin and tetrabenzporphin, where there is some overlapping of $\pi-\pi^*$ transitions, it seems likely that it is indeed underlying $n-\pi^*$ transitions that are responsible. The experimental spectrum of MgTAP in methanol shows bands at 39000 cm^{-1} and 44000 cm^{-1} [14b] which are indicated in Fig. 3. The second of these has no theoretical counterpart in the $\pi-\pi^*$ spectrum.

d) Phthalocyanine

Phthalocyanine energy levels, including those derived from vapor phase spectra of ZnPc and CuPc [18], are given in Fig. 4. An important experimental feature is the very high intensity of the Q band and the broadness of the B bands. The broad band at 3025 Å (33060 cm^{-1}) is probably the N band predicted to be at 35800 cm^{-1}. The f_2 calculation reported in Fig. 4 is in reasonably good agreement with the data, while the f_1 sum is grossly high. The energies of the stronger calculated transitions are in good agreement with the experimental values for the N, L, and C bands. As in TAP, the broadness of the B bands can be explained as due to underlying $n-\pi^*$ transitions [16]. Also, as shown in Fig. 9, there are forbidden $\pi-\pi^*$ transitions in the B region that may help to explain the broadness.

The cumulative absorption intensity plot for phthalocyanine is given in Fig. 5. There is more consistency here between the various reported experimental measurements than was the case in free base porphin. Once again it is found that $\boldsymbol{\Pi}^2$ is a more satisfactory indicator of intensity than $\boldsymbol{R}^2$.

An interesting feature of our calculations is the partial verification of the suggestion of Schechtman [15] that the benzene rings of phthalocyanine might play a semiautonomous part in determining the *uv* absorption. Schechtman assigns three peaks between 39000 and 59000 cm^{-1} to the benzenoid transitions. In Fig. 5 we see a steep rise in calculated intensity beginning at 57000 cm^{-1}. One way of deciding whether this rise is due to transitions of benzenoid character is to look at the transitions monopoles. For a one electron promotion $k \rightarrow l$, the product $C_{ik}C_{il}$ is the transition monopole and gives the contribution of atom i to the transition dipole, where C_{ik} is the MO coefficient of orbital k on atom i. The upper part of Fig. 6 shows the transition monopoles for $4e_g \rightarrow 4b_{1u}$, a typical contributing transition to the steep rise beyond 57000 cm^{-1}; the lower part of

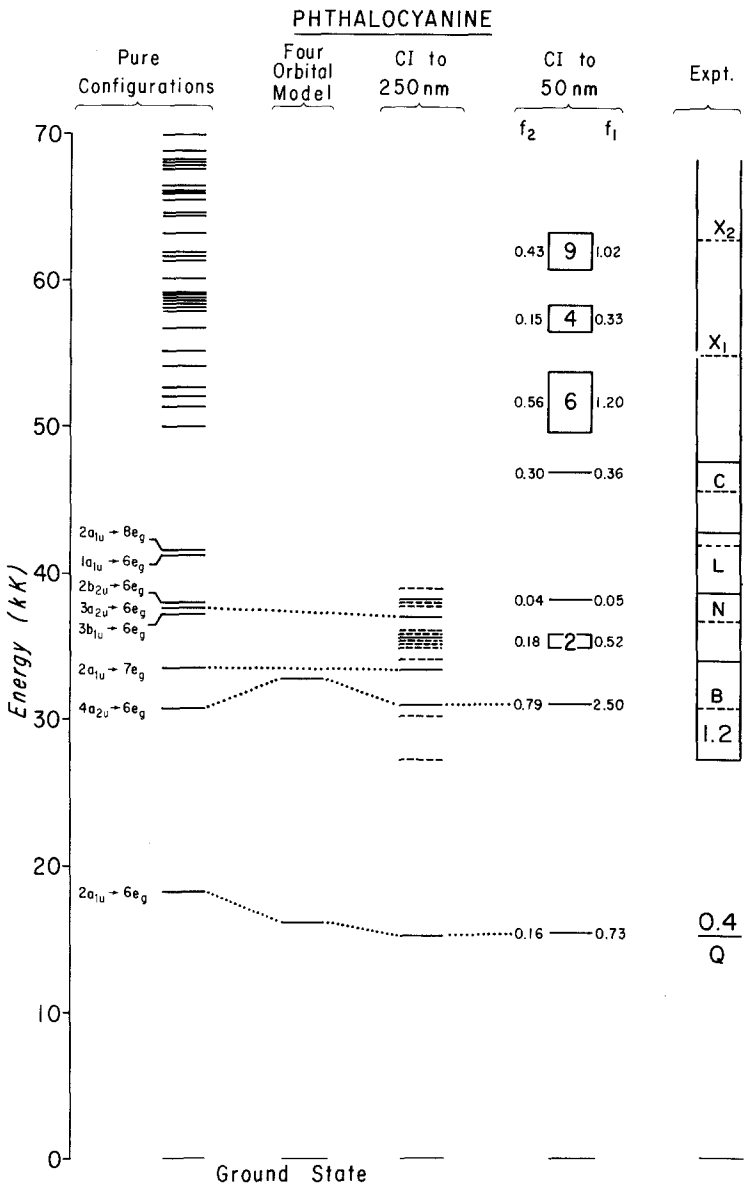

Fig. 4. See legend for Fig. 3. Forbidden levels in the region 20 to 40 kK shown as dotted lines. Experimental values based on ZnPc in vapor and solution [12a, 18b]

Fig. 6 shows the transition monopoles for $4a_{2u} \rightarrow 6e_g$ at 30570 cm^{-1}. One can see that the monopoles of the former transition are quite large on the atoms of the benzene rings, whereas the latter has monopoles overwhelmingly concentrated on the inner ring. For transitions between about 40000 and 50000 cm^{-1} we expect the excited states will be of mixed benzenoid and ring character. Beyond about 55000 cm^{-1}, benzenoid character will predominate.

e) Benzporphins

Fig. 7 shows the results of our calculations on the various benzporphin systems. Weiss *et al.* [2] reported on tetrabenzporphin (TBP), but only in the four-orbital model. To our knowledge, no previous SCMO calculation on the absorption spectrum of mono, di, or tribenzporphin has been reported. All of these should show a cluttered spectrum due to the splitting of the degeneracies of tetra-

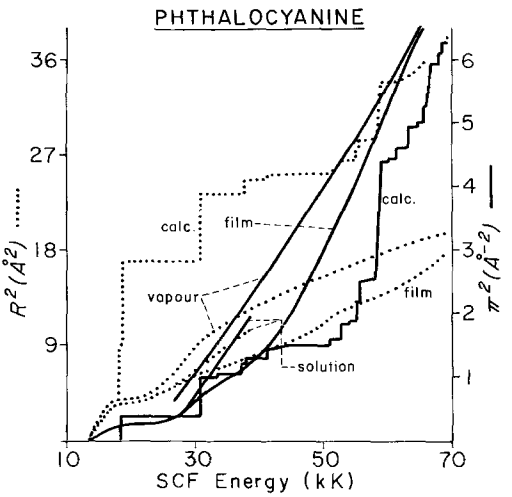

Fig. 5. Solution [14], film [15], and vapor [12] data compared with calculated values (from one-electron transitions) for $\boldsymbol{R}^2$ (dotted lines) and $\boldsymbol{\Pi}^2$ (solid lines)

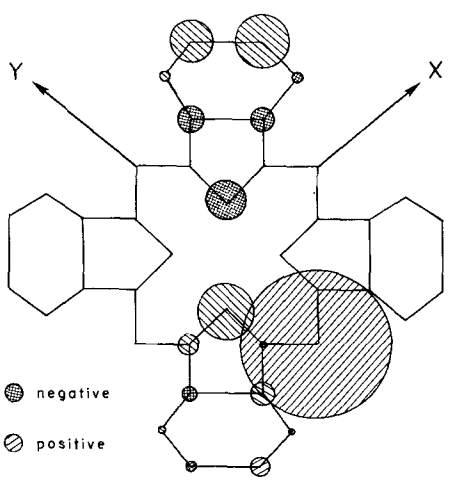

Fig. 6. Representation of $C_{ik}C_{il}$ as radius of circle about i for one-electron promotion $k \rightarrow l$. Lower part of diagram shows ring transition; upper part shows benzenoid transition (see text). Full diagrams obtained by symmetric rotation about y, antisymmetric rotation about x

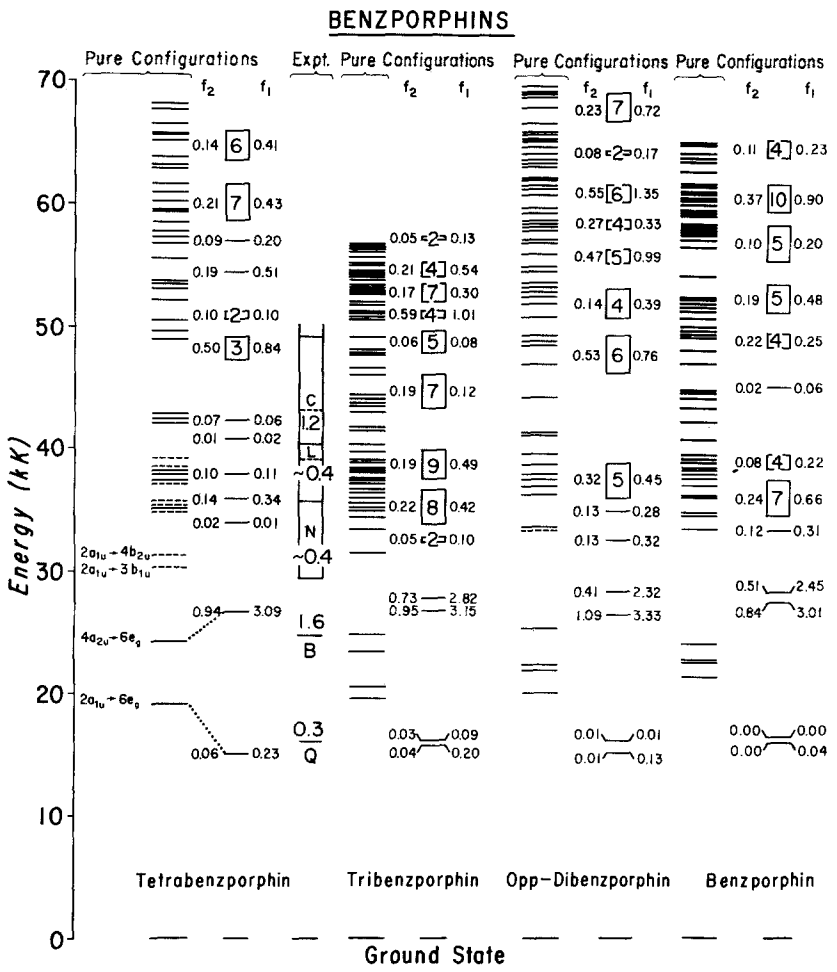

Fig. 7. See legend for Fig. 3. Experimental values for ZnTBP in vapor [12a] and octane pyridine [19]

benzporphin (TBP). All are predicted to have a greater B than Q splitting, with lower energy component in each case having greater intensity. Polarization of the bands is indicated in Table 4 given below.

Data on ZnTBP exists, and the theoretical calculation on TBP can be compared to experiment. We have recently remeasured the molar extinction coefficient in pyridine [19] and find somewhat higher values than those reported earlier [14c]. Also a weak band reported at 460 *nm* [14c] that has no theoretical counterpart has been shown by excitation spectra to be an impurity [19]. Vapor spectra have been taken down to $\lambda \gtrsim 200\ nm$ [12a]. We can determine wavelengths for all peaks in the vapor and relative f values. We can obtain absolute f values by assuming that the values for the Q and B bands measured in solution hold in vapor. The spectrum then consists of the following five bands: a clear Q band ($16000\ \text{cm}^{-1}$, $f = 0.3$), a clear B band ($24700\ \text{cm}^{-1}$, $f = 1.6$), a flattened N band

($\sim 31200\,cm^{-1}$, $f \sim 0.4$), a fairly clear L band ($39400\,cm^{-1}$, $f \sim 0.4$), and a clear C band ($43400\,cm^{-1}$, $f \sim 1.2$.) We use "C" for this last band because of its relatively high intensity.

Let us now compare the data with the calculations. The calculated energies for the Q and B bands agree well with experiment, as shown in Fig. 7. The calculated f_2 values for Q and B sum to 1.0, which must be doubled *(vide ante)* to compare to the observed f sum of 1.9. Somewhat more than in the case of phthalocyanine, the f value of Q is underestimated by f_2, while the f value of B is overestimated. However the sum of the f_2 values for both bands agrees with the experimental sum value, while f_1 is high by a factor of 3.5. The experimental N band we identify with the two calculated transitions at $37000\,cm^{-1}$ with $f_2 = 0.14$ and 0.10; the L band with the two transitions near $42000\,cm^{-1}$ with $f_2 = 0.01$ and 0.07; the C band with the three transitions around $48000\,cm^{-1}$ with $f_2 = 0.50$. Again these f_2 values must be doubled before comparing to experiment. This identification puts all experimental energies somewhat below the calculated ones. As in phthalocyanine, TBP transitions in the 48000 to $54000\,cm^{-1}$ range are benzenoid in character. A notable point in the calculations is the far greater calculated intensity in phthalocyanine and TBP above $50000\,cm^{-1}$ than in porphin and TAP. This intensity is attributable to the benzenoid transitions [15], and the data so far confirm this prediction [17, 15, 18b].

3. Calculations for Magneto-Optical Effects

a) Theory

Porphyrins and phthalocyanines are known to show large magneto-optical effects. Shashoua [20] reported on Faraday rotation, and Dratz [21] has measured magnetic circular dichroism. Malley, Feher, and Mauzerall [22] have reported Zeeman splitting. All of these observed effects are attributed to orbital angular momentum effects in the porphyrin and phthalocyanine excited states [4, 23]. In this section we use the SCMO–PPP–CI wavefunctions to calculate these values.

We shall begin from the general treatment of Stephens *et al.* [4]. For a nondegenerate ground state, the magneto-optical effects for the transition $a \rightarrow j$ are determined by two parameters $A(a \rightarrow j)$ and $B(a \rightarrow j)$. The first term arises only for degenerate excited states, while the second arises in both degenerate and nondegenerate cases. Among the effects produced is magnetic circular dichroism (MCD), which we shall emphasize in our discussion. In this phenomenon there is an enhancement in the absorption of left circularly polarized light over right or vice versa. The types of circular dichroism that arise are shown in Fig. 8. We shall discuss the sign convention more fully below.

Stephens *et al.* express $A(a \rightarrow j)$ and $B(a \rightarrow j)$ in terms of complex wave functions. For computational purposes real wave functions are more convenient. We shall assume the molecule has at least C_{2v} symmetry, so that x and y polarized states have distinct symmetry, and shall consider interaction between a diamagnetic

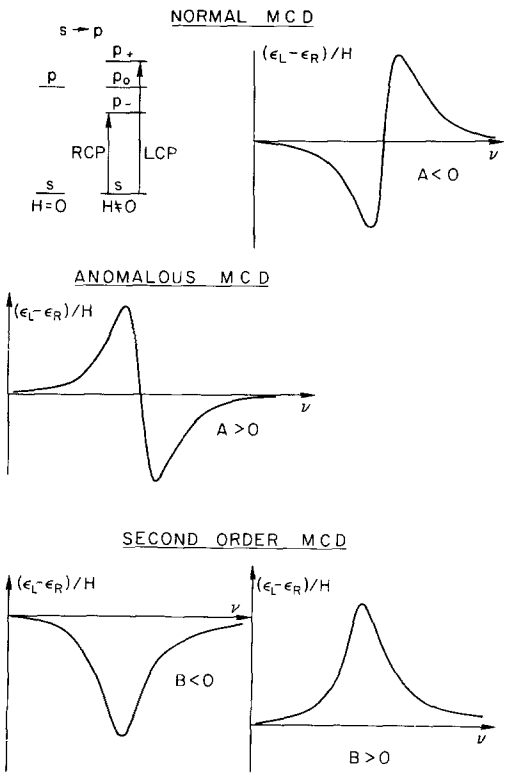

Fig. 8. Types of circular dichroism. Top panel shows $s \rightarrow p$ transition and normal MCD for degenerate states. Middle panel shows anomalous MCD for degenerate states. Bottom panel shows the two possible results of second order magnetic interactions. The quantity $[\theta]_M = 3300(\varepsilon_L - \varepsilon_R)/H$. See Ref. [26]

ground state $|a\rangle$ and a set of real excited states $|x_i\rangle$ (subscripts i and j) and $|y_k\rangle$ (subscripts j and k). For $\boldsymbol{m}$, the transition dipole operator, we shall define

$$\begin{aligned} \langle a|\boldsymbol{m}|x_i\rangle &\equiv eR_{xi}\hat{\boldsymbol{i}} \\ \langle a|\boldsymbol{m}|y_k\rangle &\equiv eR_{yk}\hat{\boldsymbol{j}} \\ \langle x_i|\boldsymbol{L}_z|y_k\rangle &\equiv i\hbar M_{ik} = -\langle y_k|\boldsymbol{L}_z|x_i\rangle . \end{aligned} \tag{3}$$

In this, $\boldsymbol{L}_z$ is the angular momentum component parallel to the unit vector $\hat{\boldsymbol{k}}$ where $\hat{\boldsymbol{i}}x\hat{\boldsymbol{j}} \cdot \hat{\boldsymbol{k}} = 1$. M_{ik} is real but its sign depends on the arbitrarily determined phases of $|x_i\rangle$ and $|y_k\rangle$. However, the triple $R_{xi}M_{ik}R_{yk}$ has a definite sign which is experimentally observable.

For a molecule with symmetry D_{2h} or lower, the term $A(a \rightarrow j)$ does not exist. The term $B(a \rightarrow j)$, which arises from the coupling of non-degenerate states by the magnetic field, consists of terms with energy denominators $W_k - W_i$ or $W_j - W_a$. In this i, j, k refer to excited states; a to the ground state. We shall in this paper neglect terms with the much larger denominators $W_j - W_a$ and keep

only the former terms. Thus from Stephens *et al.* more general expression we derive

$$B(a\rightarrow i)=e^2\beta\sum_k R_{xi}M_{ik}R_{yk}(W_k-W_i)^{-1}\,, \tag{4a}$$

where β is the Bohr magneton. We note that the subscript i refers to an x polarized state and k to a y polarized one. For y polarized states we derive

$$B(a\rightarrow k)=e^2\beta\sum_i R_{yk}M_{ik}R_{xi}(W_i-W_k)^{-1}\,. \tag{4b}$$

We note that if there is only one state $|x_i\rangle$ and one state $|y_k\rangle$ then $B(a\rightarrow i)=-B(a\rightarrow k)$, as is expected.

For a molecule where the z axis is a symmetry axis for a rotation group with degeneracy, the allowed states will be associated in degenerate pairs $|x_j\rangle$ and $|y_j\rangle$. In this case the $A(a\rightarrow j)$ term is

$$A(a\rightarrow j)=e^2\beta\,R_{xj}M_{jj}R_{yj} \tag{5}$$

while

$$B(a\rightarrow j)=e^2\beta\sum_{l\neq j}2R_{xj}M_{jl}R_{yl}(W_l-W_j)^{-1}\,. \tag{6}$$

In this last expression the summation is taken over all energy levels and the factor of two takes account of degeneracy.

When making comparisons between theory and experiment, it is common to divide $A(a\rightarrow j)$ and $B(a\rightarrow j)$ by the dipole strength. Again we follow Stephens *et al.* [4] and define the dipole strength for the non-degenerate case as

$$D(a\rightarrow i)=e^2R_{xi}^2 \tag{7}$$

and obtain the expression for x polarized states

$$\frac{B(a\rightarrow i)}{D(a\rightarrow i)}=\beta\sum_k M_{ik}(R_{yk}/R_{xi})\,(W_k-W_i)^{-1}\,. \tag{8a}$$

Similarly for y polarized states

$$\frac{B(a\rightarrow k)}{D(a\rightarrow k)}=\beta\sum_i M_{ik}(R_{xi}/R_{yk})\,(W_i-W_k)^{-1}\,. \tag{8b}$$

In the degenerate case we note that $D(a\rightarrow j)=2e^2R_{xj}^2=2e^2R_{yj}^2$ so that

$$\frac{2A(a\rightarrow j)}{D(a\rightarrow j)}=\beta M_{jj}(R_{yj}/R_{xj}) \tag{9}$$

while

$$\frac{B(a\rightarrow j)}{D(a\rightarrow j)}=\beta\sum_{l\neq j}M_{jl}(R_{yl}/R_{xj})\,(W_l-W_j)^{-1}\,. \tag{10}$$

The terms B/D and $2A/D$ are experimental observables, where the A and B values are determined either from MCD or from MORD (magnetic optical rotatory dispersion) and D is determined from the absorption coefficient. A convenient way to express the results of our calculations is in terms of dimensionless quantities

$$\begin{aligned}\mathscr{M}_{ik}^{(x)}&\equiv M_{ik}(R_{yk}/R_{xi})\\ \mathscr{M}_{ik}^{(y)}&\equiv M_{ik}(R_{xi}/R_{yk})\,.\end{aligned} \tag{11}$$

For an x polarized state the B/D term is simply $\beta \sum_k \mathscr{M}_{ik}^{(x)} (W_k - W_i)^{-1}$. From a matrix of $\mathscr{M}_{ik}^{(x)}$ one can see how strongly this series will converge. Moreover, one can use either experimental or theoretical energy denominators. Similarly for a y polarized state $B/D = \beta \sum_i \mathscr{M}_{ik}^{(y)} (W_i - W_k)^{-1}$. In the case of degeneracy it is easy to show that $\mathscr{M}_{ik}^{(x)} = \mathscr{M}_{ki}^{(y)}$ so that B/D sums are the same for both components, while $2A/D = \beta \mathscr{M}_{jj}^{(x)} = \beta \mathscr{M}_{jj}^{(y)}$. Thus it is necessary to tabulate only one of these matrices. The Zeeman splitting of an orbitally degenerate state will be $2\mathscr{M}_{jj}^{(x)} \beta H_z$, where H_z is the magnetic field along the z axis.

The method of calculation for the SCMO–PPP–CI states is relatively straightforward. The excited states are taken as a sum of singly excited states. For singlet states $\psi(v \to n)$ and $\psi(\mu \to m)$ we have $\langle \psi_a | \boldsymbol{m} | \psi(v \to n) \rangle = 1/\sqrt{2} \langle v | \boldsymbol{m} | n \rangle$

$$\langle \psi(v \to n) | \boldsymbol{L}_z | \psi(\mu \to m) \rangle = \delta_{v\mu} \langle n | l_z | m \rangle + \delta_{mn} \langle v | l_z | \mu \rangle . \tag{12}$$

Combination of these one-electron integrals with the CI expansion coefficients yields values of M_{ik}, R_{xi}, R_{yk}, from which $\mathscr{M}_{ik}^{(x)}$ and $\mathscr{M}_{ik}^{(y)}$ are determined.

The most important terms for $\mathscr{M}_{ik}^{(x)}$ are the orbital l_z values. It is simple enough to show that

$$\langle n | l_z | m \rangle = \sum_a \sum_{a<b} (C_{na} C_{mb} - C_{nb} C_{ma}) \langle \chi_a | l_z | \chi_b \rangle \tag{13}$$

where C_{nb}, etc., are the expansion coefficients of the molecular orbital n onto the π atomic orbital χ_b on center b. The integral on the atomic orbitals can further be written [4, 24]

$$\langle \chi_a | l_z | \chi_b \rangle = -i\hbar T(a, b) [\xi_a \eta_b - \eta_a \xi_b] \tag{14}$$

where (ξ_a, η_a) and (ξ_b, η_b) are the x, y coordinates of the two centers in a.u. $T(a, b)$ has a form like an overlap integral and is given in Appendix 1 for equal and unequal exponents. We used exponents of 1.5679 for carbon and 1.9170 for nitrogen.

Table 2. Orbital zeeman terms[a]

Compound	Top filled $\hbar^{-1}(a_{1u} \lvert l_z \rvert a_{2u})$	Lowest empty $\hbar^{-1}(e_{gx} \lvert l_z \rvert e_{gy})$
Porphin	2.27	2.09
(Simple Hückel)[b]	(1.67)	(1.29)
(Extended Hückel)[c]	(2.37)	(2.39)
TAP	2.17	1.90
TBP	1.99	1.92
Pc	2.12	1.82
H_2 Porphin	2.24	2.08
Chlorin	2.06	1.84
Bacterio	2.05	2.03
MBP	2.05	1.95
OPP–DBP	2.03	1.96
TRIBP	1.99	1.92

[a] Symmetry labels apply to D_{4h} systems. Analogous orbitals chosen for molecules of lower symmetry. Orbital phases chosen to give positive values.

[b] Obtained with $\alpha_N = \alpha_C$. See Ref. [34]. Only nearest neighbor l_z integrals included.

[c] See Ref. [35]. All two center l_z integrals included.

Only nearest neighbor integrals were included to be consistent with the zero differential overlap assumption inherent in the PPP wavefunctions. In Table 2 we have tabulated the orbital angular momentum integrals for top filled and lowest empty orbitals. These are the largest such integrals, but the others are not negligible.

b) Degenerate Case $A(a \rightarrow j)$ Term

The four D_{4h} molecules are presented in Table 3. The diagonal entries are $\mathscr{M}_{jj}^{(x)} = 2\beta^{-1} A/D$. The sign is a genuine observable. To clarify it we shall use as a reference an atomic transition $s \rightarrow p$. In a magnetic field the energy levels for $m = \pm 1, 0$ will be shifted by $\pm \beta H, 0$. For light incident parallel to H, only transitions to $\pm \beta H$ occur. The transition to $m = +1$ requires left circularly polarized light, by which we mean the electric vector portrays a right-hand helix [25a][1]. The transition to $m = -1$ requires right circularly polarized light. The expected circular dichroism is shown in Fig. 8. By our convention $\mathscr{M}_{jj}^{(x)} = -1$ and $A < 0$ for $s \rightarrow p$. It is convenient in D_{4h} cases to refer to bands with $A < 0$ as "normal MCD" and cases with $A > 0$ as "anomalous MCD."

We shall here consider whether normal or anomalous MCD occurs in the Q(0, 0) and B(0, 0) bands of D_{4h} porphyrin. We note that Table 3 predicts normal MCD for all Q(0, 0) bands and for all B(0, 0) bands except unsubstituted porphin. Experimentally $A < 0$ has been found for all Q(0, 0) and B(0, 0) bands that have been investigated in D_{4h} cases [4, 22, 26, 27]. This includes octalkylporphin, tetraphenylporphin, porphin, and phthalocyanine. (Although Dratz [21] reported anomalous MCD in metalloporphyrins, he did not determine sign absolutely, and we believe he erred on this point.) We are not disturbed that the B(0, 0) band of metalloporphyrins so far studied show $A < 0$, although Table 3 predicts $\mathscr{M}_{BB}^{(x)} = +0.030$. This small value is essentially a difference between the MO contributions of top filled and lowest empty orbitals (Table 2) plus many small terms. It might vary quite strongly with small changes of parametrization. That the B band is sensitive to parametrization has been shown by the calculations of Stephens *et al.* [28] on triphenylene and coronene B bands. Sooner or later a D_{4h} porphyrin may be found with substituents such that $A > 0$ for the B band.

Table 3. Matrix of $\mathscr{M}_{ik}^{(x)}$ value for (Porphin, TAP/TBP, Phthalocyanine)[a] and dipole strengths

R_{xi}^2(Å^2)			Q_y		B_y		N_y		L_y	
0.012	0.971	Q_x	−4.347	−3.835	6.109	0.584	−4.812	2.527	−1.130	0.198
1.421	4.412		−3.684	−3.134	2.133	1.768	0.035	0.0163	−0.001	0.091
9.154	3.809	B_x	0.008	0.147	0.030	−0.258	0.141	0.014	0.144	0.400
10.710	7.519		0.283	1.077	−0.275	−0.632	0.003	0.013	0.165	0.013
0.982	5.308	N_x	−0.063	0.464	1.396	0.011	0.302	0.376	−1.256	−0.274
0.032	0.012		1.546	−2.766	−0.734	−6.362	1.752	−1.236	−0.693	−1.833
0.380	0.290	L_x	−0.036	0.663	3.485	5.247	−3.048	−5.021	−0.043	−0.020
0.022	0.166		−0.022	1.893	1.657	0.573	−1.038	0.148	1.141	1.301

[a] Order of entries in Table: Porphin, TAP top line; TBP, phthalocyanine lower line. Thus $\mathscr{M}_{QQ}^{(x)} = -4.347$, $\mathscr{M}_{QB}^{(x)} = 6.109$, and $\mathscr{M}_{BB}^{(x)} = 0.030$ for porphin.

[1] We might note that an opposite definition for left circularly polarized light has been given [25b].

The absolute magnitude of $\mathscr{M}_{QQ}^{(x)}$ calculated for porphin can be compared to the experimental MCD numbers of Dratz [21]. He studied six metal deuteroporphyrins and obtained values from 4.44 for the cobalt complex to 6.52 for the zinc complex, a range of variation he can explain by perturbation theory. Stephens *et al.* [28] analyzing zinc hematoporphyrin MORD find 6.94. For zinc coproporphyrin by MCD Dratz obtains 6.5 ± 0.5. On this same compound Malley *et al.* [22] by direct Zeeman studies obtain 9.5 ± 0.6 at room temperature and 6.4 ± 0.6 at 77° K. Recently Sutherland *et al.* [29] have explained the discrepancy between the MCD value and the direct Zeeman value by postulating a zero-field splitting of the orbital degeneracy and an inequality of the two transition dipoles. According to this explanation, the MCD value should be a more accurate measurement of the orbital Zeeman splitting. Our calculated value of 4.35 agrees reasonably well with the measured MCD value of cobalt deuteroporphyrin.

Can our calculated magnitude of 4.35 be raised while retaining a reasonable set of parameters? The basic ingredients for the calculation are: (i) the coefficients of the π electron wavefunction, (ii) the exponents of the atomic orbitals, and (iii) the molecular geometry. Several calculations for orbital angular momentum were carried out using other sets of MO coefficients. (Two such calculations for porphin are shown in Table 2.) In no case did we obtain values significantly larger than those listed. The atomic orbitals affect $T(a, b)$, which is maximized by an orbital exponent of $\zeta = 1.3$. Use of such a smaller exponent agrees with the double-zeta carbon $2p_z$ orbital of Clementi [30] and has been justified in another context by Silverstone *et al.* [31]. This could raise $\mathscr{M}_{QQ}^{(x)}$ by about 10%. If all bond lengths are reduced by 0.06 Å another increase of 10% can be obtained. All effects taken together would be unlikely to increase $\mathscr{M}_{QQ}^{(x)}$ much above 5.5 to 6. This agrees with the larger MCD values of Dratz and supports the conclusion of Sutherland *et al.* [29] that the room temperature Zeeman value of Malley *et al.* [22] is high.

Experimental comparison can also be made between the calculated value $\mathscr{M}_{QQ}^{(x)} = -3.134$ for phthalocyanine (Pc) and values obtained from experiment. Stephens *et al.* [4] analyzed Shashoua's MORD data on MgPc [20] and obtained $\mathscr{M}_{QQ}^{(x)} = -8.16$. Pershan *et al.* [23] analyzed Shashoua's MORD data on ZnPc and obtained a value of -1.3, an enormous discrepancy. We have carefully reconsidered the Pershan *et al.* calculation and found errors in the values for magnetic molar rotation and angular frequency halfwidth. With correct values $\Phi_s(\max) = -5.95 \times 10^{-3}$ cm^3/gauss mole and $\Gamma = 6.1 \times 10^{13}$/sec, a value of $\mathscr{M}_{QQ}^{(x)} = -1.9$ is obtained. (For definitions of $\Phi_s(\max)$ and Γ, see Ref. [23].) A further correction of $\pi/2$ arises from the Pershan *et al.* assumption of Lorentzian shape, giving $\mathscr{M}_{QQ}^{(x)} = -3.0$[2]. However the remaining difference arises from the data. Comparison of MgPc with ZnPc shows that both have similar values for D, while MgPc has a value of $\Phi_s(\max)$ that is 0.88 times the ZnPc value, and a line width 1.75 times that ZnPc value. From the Pershan *et al.* formulas we expect $\mathscr{M}_{QQ}^{(x)} = -3.0 \times 0.88 \times (1.75)^2 = -8.1$. The data show that CuPc also has a comparable value of D, a value of $\Phi_s(\max)$ that is only 0.24 times the ZnPc value, and a linewidth 1.3 the ZnPc value. Thus we roughly expect $\mathscr{M}_{QQ}^{(x)} = -3.0 \times 0.24 \times (1.3)^2 = -1.2$. Thus analysis of the Shashoua data gives $\mathscr{M}_{QQ}^{(x)} = -8.1$, -3.0, and -1.2

[2] With a Lorentzian line shape $\int \varepsilon(\omega)\, d\omega = \pi \varepsilon(\max)\, \Gamma/2$; however experimental shapes are such that $\varepsilon(\max)\, \Gamma$ is a better estimate of integrated intensity.

for McPc, ZnPc, and CuPc respectively, all of which should be -3.1 according to our calculations.

This range of values cannot be explained by perturbation theory such as that used by Dratz [21] for the metal prophyrins. The broad band of MgPc suggests peculiar complexing phenomena are occurring. Such phenomena are not explicitly considered in the theory of band shape used to extract the value of $\mathscr{M}_{QQ}^{(x)}$ from MORD data. We tend to believe that the naive treatment of band shape has led to an incorrect "experimental" value of $\mathscr{M}_{QQ}^{(x)}$ for MgPc. More experiments on phthalocyanine varying metal, solvent, and temperature are needed. We also need more theoretical analyses, such as that of Sutherland *et al.* [29], on how solvent effects on band shape and how orbital degeneracy will affect the $\mathscr{M}_{QQ}^{(x)}$ values extracted from the data.

c) Degenerate Case $B(a \rightarrow j)$ Term

The value of $\beta^{-1}B/D = \sum_k \mathscr{M}_{ik}^{(x)} (W_k - W_i)^{-1}$. As can be seen from Fig. 8, the sign of this quantity is an observable. Thus for the Q band where $A < 0$, a value $B < 0$ will enhance the longwavelength minimum while $B > 0$ will enhance the shortwavelength maximum. Our calculation for the Q state of porphin (Table 3) shows that interaction with the B state gives a positive contribution to the sum while the N state gives a negative contribution about half the size. The net positive contribution should enhance the shortwavelength maximum.

The experimental information is ambiguous. Dratz [21] finds different results for different systems: The longwavelength Q band dichroism is enhanced for Zn coproporphyrin III, Fe (II) protoporphyrin IX in H_2O, bovine oxyhemoglobin, cytochrome *c*; while the shortwavelength is enhanced for Ni, Cu, Zn deuteroporphyrin IX and Fe (III) protoporphyrin IX in pyridine. The experimental sign of the B term thus appears to be quite variable. As a sum of terms from many states, this is not so surprising. Because the energy denominators are several thousand wavenumbers, the overall magnitude of $\beta^{-1}B/D \sim 10^{-3}$ cm. Stephens *et al.* [4] determined an experimental value of -3.9×10^{-3} cm for Zn hematoporphyrin, which by the above arguments means enhanced longwavelength dichroism, although their experimental data showed enhanced shortwavelength dichroism. They report the impossibly large value of -72×10^{-3} cm for MgPc. As suggested above, the value $\mathscr{M}_{QQ}^{(x)} = -8.1$ obtained for MgPc is far too large in magnitude when compared to theory and seems due to an inadequate treatment of the anomalously large bandwidth. We believe that the impossibly large value for $\beta^{-1}B/D$ comes from this same inadequacy.

As noted in the previous paragraph, a non-zero B value when added to a non-zero A value can give asymmetry to the MCD curve of degenerate molecules, even though there is no lifting of degeneracy. Sutherland *et al.* [29] note that if the x and y transition dipoles are not equal and there is zero field splitting, a similar asymmetry will occur. Thus experimentally observed asymmetries may be due to this effect as well as to non-zero $\beta^{-1}B/D$, and extraction of $\beta^{-1}B/D$ from the data must proceed with caution.

d) Non-Degenerate Case B(a→j) Terms

The results for the non-degenerate molecules are given in Table 4. The axis convention is given in Fig. 9. These systems are closely related to the degenerate systems given in Table 3. This relation is manifest in Table 2, which shows that the

Table 4a. Matrix of $\mathscr{M}_{ik}^{(x)}$ values for (free base porphin, chlorin/bacteriochlorin, MBP/OPP-DBP, TRIBP)[a,b] and dipole strengths

R_{xi}^2(Å^2)			Q_y		B_y		N_y		L_y	
0.077	0.143	Q_x	0.635	−0.133	−0.477	5.371	−0.575	0.082	−0.857	−0.247
0.573	0.020		−8.702	−13.976	5.283	7.048	0.035	0.038	0.126	0.124
0.049	0.536		15.820	− 5.606	9.272	3.201	0.989	−0.004	0.306	0.003
5.584	7.500	B_x	−0.014	0.135	−0.279	−0.406	0.448	−0.020	0.089	0.033
1.963	10.169		1.431	− 0.010	−0.101	−0.113	−0.153	−0.001	−0.046	0.060
11.687	10.951		−0.010	0.122	−0.121	0.136	0.057	−0.173	0.085	−0.007
5.211	0.697	N_x	0.010	−0.695	0.833	−1.327	−0.451	−0.016	0.048	0.015
5.580	0.014		0.068	0.219	−0.428	10.211	0.046	−0.006	0.033	−12.885
0.903	0.172		0.655	−0.066	0.587	−2.470	0.290	0.557	0.234	0.024
0.254	0.514		0.017	−0.291	2.185	−1.207	0.205	0.028	−2.506	−0.683
0.016	0.866	L_x	4.876	0.337	−4.785	0.616	−1.812	−0.010	1.745	0.370
0.744	0.099		0.283	0.373	2.464	2.236	−1.145	−0.139	−0.654	0.236
$E^{(y)}$			16.91	16.17	28.79	28.75	35.01	32.54	38.42	35.68
(calc.)			14.93	15.89	32.57	28.16	43.28	32.59	43.77	34.29
			15.12	15.69	28.33	27.61	35.82	30.67	36.97	33.59

[a,b] See footnotes for Table 4b.

Table 4b. Matrix of $\mathscr{M}_{ik}^{(y)}$ values for (free base porphin, chlorin/bacteriochlorin, MBP/OPP-DBP, TRIBP)[a,b] and dipole strengths

R_{yi}^2			Q_x		B_x		N_x		L_x	
0.0017	0.802	Q_y	28.956	−1.624	−45.813	1.266	29.674	−0.603	2.519	−0.187
3.238	0.250		−1.539	−1.119	0.867	−0.413	0.118	0.012	0.025	1.168
0.820	1.187		−0.952	−2.530	−0.133	1.252	0.722	−0.010	0.257	0.031
9.807	7.473		−0.004	0.102	−0.159	−0.407	0.442	−0.124	0.057	−0.083
8.244	8.031	B_y	0.367	0.018	−0.024	−0.143	−0.289	0.017	−0.009	0.066
7.565	9.417		0.060	0.182	−0.187	−0.201	0.070	−0.045	0.242	0.023
0.489	0.106	N_y	−0.089	0.110	5.019	−1.387	−4.716	−0.106	0.105	0.136
0.025	0.003		0.808	0.232	−12.168	−3.418	10.284	−0.024	−1.196	−2.636
0.272	0.008		0.179	−0.281	2.463	−9.025	0.964	11.382	−3.131	−1.630
0.379	0.189	L_y	−0.174	−0.186	1.322	1.310	0.658	0.054	−1.680	−1.859
0.056	0.434		1.297	0.006	−1.575	1.396	3.330	−0.402	0.513	0.739
0.290	0.001		0.052	1.609	3.433	−10.172	0.729	3.749	−1.682	21.308
$E^{(x)}(kK)$			14.99	17.71	27.52	28.58	31.67	32.84	40.18	35.19
(calc.)			17.12	16.38	30.23	27.26	32.00	31.71	48.35	33.15
			15.92	15.92	26.27	26.55	32.45	32.21	34.86	32.60

[a] Order of entries in Table indicated by slashes as for Table 3. Free base uses $\Delta\alpha = 5.5$ eV.

[b] Abbreviations: MBP (monobenzporphin); OPP–DBP (opposite dibenzporphin); TRIBP (tribenzporphin).

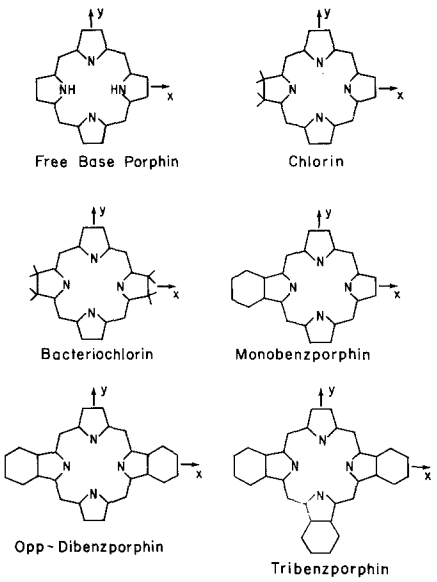

Fig. 9. Orientation of molecules of D_{2h} and C_{2v} symmetry

angular momenta of top filled and lowest empty orbitals is much the same for all systems. Nonetheless the absolute values of $\beta^{-1}B/D$ can be quite different for two quasidegenerate bands. Thus for chlorin Q_x and Q_y we get:

$$10^3\beta^{-1}B/D[Q_y] = -1.624\,(1.54)^{-1} + 1.266\,(12.41)^{-1} - 0.603\,(15.50)^{-1} - 0.187\,(19.02)^{-1} = -1.001\text{ cm},$$

$$10^3\beta^{-1}B/D[Q_x] = -9.133\,(-1.54)^{-1} + 5.371\,(11.04)^{-1} + 0.082\,(14.83)^{-1} - 0.247\,(17.97)^{-1} = 6.409\text{ cm}.$$

We see from these calculations and Fig. 9 that the longwavelength Q_y transition should show RCP (right circular polarization) while the shorter wavelength Q_x band should show LCP. The main contribution arises from the magnetic interaction between Q_y and Q_x, although the other terms are not negligible.

In analogy to our earlier definition of normal and anomalous MCD in D_{4h} systems, it is convenient to call RCP ($B<0$) "normal longwavelength MCD" and LCP ($B>0$) "anomalous longwavelength MCD" in systems of D_{2h} or lower symmetry. Examination of Table 4 shows that all the D_{2h} molecules except free base porphin are calculated to show normal longwavelength MCD. However measurements of the free bases of octalkylporphin, tetraphenylporphin, and unsubstituted porphin [21, 26, 27b] do show normal longwavelength MCD. On the other hand measurements of the dication and the free base of tetraphenylchlorin show anomalous longwavelength MCD [27b]. This is the reverse of the predictions in Table 4. The sign of longwavelength MCD in molecules of D_{2h} or lower symmetry depends quite delicately on the wavefunctions. In the next section we take up this problem.

Table 5. Transition gradient and oscillator strength for chlorin and bacteriochlorin[a]

State Energy	(kK)	$\Pi_x(\text{Å})^{-1}$	$\Pi_y(\text{Å})^{-1}$	f_2
A. Chlorin				
Q_y	16.17		0.105	0.028
Q_x	17.71	−0.019		0.001
B_x	28.58	0.610		0.534
B_y	28.75		−0.638	0.580
N_y	32.54		−0.100	0.013
N_x	32.84	0.261		0.085
L_x	35.19	−0.233		0.063
L_y	35.68		0.176	0.036
B. Bacteriochlorin[a]				
Q_y	14.93		0.138	0.052
Q_x	17.12	0.062		0.009
B_x	30.23	0.285		0.110
N_x	32.00	0.599		0.460
B_y	32.57		0.731	0.673
N_y	43.28		0.021	0.001
L_y	43.76		0.109	0.011
L_x	48.35	0.066		0.004

[a] Opposite tetrahydroporphin.

e) Further Discussion of Normal and Anomalous MCD

A considerable insight into the observed MCD of porphyrins and related systems can be obtained by discussing the basis of normal and anomalous MCD in degenerate systems and normal and anomalous longwavelength MCD in non-degenerate systems.

The fact that Q(0′, 0″) bands in D_{4h} porphyrins must show normal MCD can be understood as follows. The phase of the wavefunctions can be chosen so that

$$\begin{aligned} C_4 Q_x &= Q_y \\ C_4 Q_y &= -Q_x \end{aligned} \tag{15}$$

where C_4 is a rotation that sends the x axis into the y axis. In this case $\mathrm{M}(Q_x, Q_y)$ defined as

$$i\hbar \mathrm{M}(Q_x, Q_y) = \langle Q_x | L_z | Q_y \rangle \tag{16}$$

will be a negative number ~ -2 to -4. With this choice of phase for the wavefunctions, the transition dipoles

$$\begin{aligned} \langle a | e\boldsymbol{r} | Q_x \rangle &= eR_x \hat{\boldsymbol{i}} \\ \langle a | e\boldsymbol{r} | Q_y \rangle &= eR_y \hat{\boldsymbol{j}} \end{aligned} \tag{17}$$

must relate as

$$\begin{aligned} C_4 R_x \hat{\boldsymbol{i}} &= R_y \hat{\boldsymbol{j}} \\ C_4 R_y \hat{\boldsymbol{j}} &= -R_x \hat{\boldsymbol{i}} . \end{aligned} \tag{18}$$

The consequence of Eqs. (18) is that either R_x, R_y are both positive or are both negative. The triple $R_x \mathrm{M}(Q_x, Q_y) R_y < 0$. This triple determines that the sign of $A < 0$. For the B(0′, 0″) band Eqs. (18) still hold on symmetry grounds. However as already noted [*vide ante*] the value of $\mathrm{M}(B_x, B_y)$ defined by an equation analogous

to Eq. (16) is the difference between two numbers of comparable size. The difference might make $M(B_x, B_y)$ a small positive number giving rise to anomalous MCD.

What will be the A value for vibrational overtones of the Q and B bands of degenerate porphyrins? Although Stephens *et al.* [4] noted that $\mathscr{M}_{jj}^{(x)} = 2\beta^{-1}A/D$ should have the same magnitude for vibrational bands $Q(v', 0'')$ as for the $Q(0', 0'')$ band, they failed to note, that the sign of $\mathscr{M}_{jj}^{(x)}$ depends on the symmetry of the vibration, a fact noted elsewhere [32]. It can be shown by group theory that the transition dipoles $R_x(v', 0'')$, $R_y(v', 0'')$ will transform according to Eq. (18) if v' is a vibration of α_{1g} or α_{2g} symmetry but will transform as

$$\begin{aligned} C_4 R_x(v', 0'')\,\hat{\boldsymbol{i}} &= -R_y(v', 0'')\hat{\boldsymbol{j}} \\ C_4 R_y(v', 0'')\,\hat{\boldsymbol{j}} &= R_x(v', 0'')\,\hat{\boldsymbol{i}} \end{aligned} \tag{19}$$

if v' if of β_{1g} or β_{2g} symmetry. Eq. (19) will result in anomalous MCD. It has been noted [32] that the experimental $Q(1, 0)$ bands of metalloporphyrins are a composite of $Q(v', 0'')$ bands with several different v' vibrations [32]. It is therefore not surprising that both signs of A are observed, and MCD is complex [21, 27]. For ZnTPP the $Q(1, 0)$ shows little resolution and appears as a single $A<0$ band [26]. However, since the unresolved band has contributions with both $A>0$ and $A<0$, we can understand why the value of A/D is not as extreme for $Q(1, 0)$ as for $Q(0, 0)$.

Consider now porphyrins where substituents or free base formation break the D_{4h} symmetry. Suppose we label the lower energy transition Q_x. (The argument, of course, does not depend on choice of x instead of y.) The sign of MCD will depend mainly on $R_x M(Q_x, Q_y) R_y$, since the Q_x, Q_y magnetic interaction will be the predominant term in Eq. (4a). If the perturbation from D_{4h} symmetry is small, this term will maintain the same sign as in the D_{4h} case, *i.e.* negative. The result will be $B<0$ for the $Q_x(0', 0'')$ band, and normal longwavelength MCD will occur. Since $M(Q_x, Q_y)$ has relatively large magnitude its sign will persist as the perturbation from D_{4h} symmetry increases. However the transition dipoles are no longer symmetry related. If the symmetry is at least C_{2v} we will have

$$\begin{aligned} C_4 R_x \hat{\boldsymbol{i}} &= \eta R_y \hat{\boldsymbol{j}} \\ C_4 R_y \hat{\boldsymbol{j}} &= -\eta^{-1} R_x \hat{\boldsymbol{i}} \end{aligned} \tag{20}$$

replacing Eq. (18). If the perturbation from D_{4h} symmetry is small, η may remain close to unity as in Eq. (18). However for certain large perturbations a negative η may occur. For such a case the sign of $R_x M(Q_x, Q_y) R_y > 0$, and we will observe anomalous longwavelength MCD.

We therefore see that normal longwavelength MCD will be expected for substituted D_{2h} porphyrins such that in the compound itself and in the closest related D_{4h} compound the Q_x and Q_y bands are moderately intense. This explains the observation that the free bases of octalkylporphin [21, 27b], tetraphenylporphin [26], and phthalocyanine [27a] show normal longwavelength MCD. In unsubstituted free base porphin, although the intensity of $Q_x(0, 0)$ and $Q_y(0, 0)$ is relatively weak, the MCD remains normal [27b]. Djerassi *et al.* have found anomalous longwavelength MCD in a number of dihydroporphins (chlorins) and in some low symmetry substituted free base porphyrins [27]. We note that in chlorins the higher energy $Q_x(0, 0)$ band is usually quite weak so that a negative η

value is not so surprising. Very detailed consideration of the effect of the substituents on excited state wavefunctions will be needed to predict whether in a given case longwavelength MCD should be normal or anomalous. However theory makes clear why both behaviors can be obtained.

Some comments can be made about the sign of the B values for the vibronic bands $Q_x(v', 0'')$ and $Q_y(v', 0'')$ in cases where D_{4h} symmetry is lifted by a free base perturbation. If we assume the perturbation is too weak to substantially change the character of these states but merely lifts their degeneracy, then the B term of a band like $Q_x(v', 0'')$ will be dominated by its interaction with $Q_y(v', 0'')$. Just as $Q(v', 0'')$ bands of degenerate porphyrins can show A values of either sign depending on the symmetry of v', bands $Q_x(v', 0)$ can show B values of either sign. Alternation of sign of B values is in fact observed in different regions of the $Q_x(1, 0)$ and $Q_y(1, 0)$ bands [26, 27b]. This is expected, since it has been known that such bands contain vibrations of different symmetry. If the individual vibrational components of $Q_x(1, 0)$ and $Q_y(1, 0)$ are not resolved, the observed B/D is due to the combined effect of several vibrations and will reach a less extreme value than in the corresponding $Q_x(0, 0)$ and $Q_y(0, 0)$ bands.

Finally we note that Kobayashi *et al.* [27] find no MCD in the "Longo" band at $21\,000\,\mathrm{cm}^{-1}$. The absence of MCD could be explained for a Q(2, 0) band if it were a composite band of vibrational symmetries with cancelling B values. It could also be explained as an electronic origin with small and cancelling magnetic interactions with electronic transitions to higher and lower energy, a situation that is quite likely according to our numbers in Table 4. Thus MCD does not provide an unequivocal identification of the Longo band.

Summary

The calculations reported in this paper have given a number of results for porphyrin and some related compounds that we now summarize:

(1) For an excited state built as a linear combination of single excitations, transition gradient operators predict intensities with reasonable accuracy even though transition dipole operators predict intensities high by about a factor of three to four.

(2) The B band intensity of free base porphyrin is spread over a range of $1000\,\mathrm{cm}^{-1}$ or more. Conceivably there is a $\pi - \pi^*$ transition between $Q_y(1, 0)$ and the main Soret band in the free base.

(3) The compounds tetrabenzporphin and phthalocyanine show far stronger absorption than porphin and tetrazaporphin in the range $\lambda < 200\,\mathrm{nm}$ due to benzenoid transitions.

(4) Very likely the cause of the anomalously broad Soret absorption in tetrazaporphin and phthalocyanine compared to porphin and tetrabenzporphin is underlying $n - \pi^*$ transitions.

(5) Theory seems to be giving the correct order of magnitude for magnetic effects due to orbital angular momenta. For porphin a theoretical value of $4.35\,\hbar$ calculated for the Q state compares to experimental values from MCD between 4.4 and $6.9\,\hbar$. For phthalocyanine the "experimental" values cover the range 1.2 to 8.1, while theory is $3.1\,\hbar$. It is suggested that the "experimental" values may be in error due to improper treatment of the bandshape.

(6) The MCD for the Q(0′, 0″) of D_{4h} porphyrins must be normal, *i.e.* have $A<0$. Bands B(0′, 0″) may sometimes show $A>0$.

(7) Vibrational bands Q(v′, 0″) will have $2\beta^{-1}A/D$ values of the same magnitude as Q(0′, 0″), however $A<0$ for v′ of α_{1g} or α_{2g} symmetry (normal MCD) but $A>0$ for v′ of β_{1g} or β_{2g} symmetry (anomalous MCD). Experimental Q(1, 0) bands are composites of several Q(v′, 0″) bands with both signs of A present.

(8) In degenerate cases the value of $\beta^{-1}B/D$, which introduces asymmetry to the A term MCD, should be in the range $\pm 3\times 10^{-3}$ cm. Magnitude grossly larger than this indicate errors in the experimental analysis.

(9) In non-degenerate porphyrins where the $Q_x(0', 0'')$ and $Q_y(0', 0'')$ bands are moderately intense and the perturbation lifting D_{4h} symmetry is small, longwavelength MCD will be "normal", *i.e.* RCP. In cases where one or both bands are very weak or the perturbation lifting D_{4h} symmetry is large, the long-wavelength MCD may be "anomalous", *i.e.* LCP.

(10) Vibrational bands $Q_x(v', 0'')$ and $Q_y(v', 0'')$ in non-degenerate cases will (to zeroth order) have B values of equal magnitude and opposite sign. The absolute sign will depend on the symmetry of v′. Experimental $Q_x(1, 0)$ and $Q_y(1, 0)$ bands will contain various v′ vibrations, so both signs of B occur. The observed MCD may result from the sum of B values of both signs.

Acknowledgements. This research was supported in part by Public Health Services Grant GM 14292 from the Division of General Medical Sciences and by AEG Contract W-7405-ENG-48. One of us (MG) acknowledges fruitful discussion with Drs. V. E. Shashoua and E. A. Dratz on magneto-optical effects in porphyrins. C. W. thanks the National Institutes of Health for a post-doctoral fellowship.

Prof. C. Djerassi of Stanford University kindly supplied us with some previously unpublished MCD spectra.

Appendix 1 — $T(a, b)$

For the case of orbitals a and b having equal exponents, it can be shown [4, 24] that

$$T(a, b)=0.2\zeta^2 e^{-\varrho}[1+\varrho+(\varrho^2/3)]\,.$$

In the case of unequal exponents

$$T(a, b)=0.2\,\zeta^2 e^{-\varrho}[1+\varrho+(\varrho^2/3)]\,(1-\tau^2)^{7/2}B\,.$$

In these expressions

$$\zeta=(\zeta_a+\zeta_b)/2$$

$$\tau=(\zeta_a-\zeta_b)/(\zeta_a+\zeta_b)$$

$$\varrho=\zeta R$$

$$B=15[(\tau\varrho)^2\sinh(\tau\varrho)-3\tau\varrho\cosh(\tau\varrho)+3\sinh(\tau\varrho)]/(\tau\varrho)^5\,.$$

References

1. Gouterman, M., Wagnière, G. H.: J. molecular Spectroscopy **11**, 108 (1963), (Paper II).
2. Weiss, C., Kobayashi, H., Gouterman, M.: J. molecular Spectroscopy **16**, 415 (1965), (Paper III).
3. McHugh, A. J., Gouterman, M.: Theoret. chim. Acta (Berl.) **13**, 249 (1969).
4. Stephens, P. J., Suëtaka, W., Schatz, P. N.: J. chem. Physics **44**, 4592 (1966).
5. Mataga, N., Nishimoto, K.: Z. physik. Chem. (Frankfurt) **13**, 140 (1957).
6. Hoard, J. L., Hamor, M. J., Hamor, T. A.: J. Amer. chem. Soc. **85**, 2334 (1963).
7. Robertson, J. M., Woodward, I.: J. chem. Soc. (London) **1837**, 219.
8. Rimington, C., Mason, S. F., Kennard, O.: Spectrochim. Acta **12**, 65 (1958).

9. a Roos, B., Skancke, P. N.: Acta chem. scand. **21**, 607, (1967).
   b Fischer-Hjalmars, I., Sundbom, M.: Acta chem. scand. **22**, 607 (1967).
   c Sundbom, M.: Acta chem. scand. **22**, 1317 (1967).
   d Knop, J. V., Knop, A.: Z. Naturforsch. **25**a, 1720 (1970).
10. a Gouterman, M.: J. chem. Physics **30**, 1139 (1959).
   b Gouterman, M.: J. molecular Spectroscopy **6**, 138 (1961), (Paper I).
11. a Sevchenko, A. N., Solov'ev, K. N., Mashenkov, V. A., Shkirman, S. F.: Soviet Phys.-Dokl. **10**, 778 (1966).
   b Gurinovich, G. P., Sevchenko, A. N., Solov'ev, K. N.: Spectroscopy of chlorophyll and related compounds. (Izdatel'stvo Nauka i Tekhnika, Minsk, 1968; Eng. trans.: National Technical Information Service, U.S. Dept. of Commerce, Springfield, Virginia 22151).
12. a Edwards, L.: Ph. D. Thesis, Committee on Chemical Physics, Harvard University (1969).
   b Paper XVII: — Dolphin, D. H., Gouterman, M., Adler, A. D.: J. molecular Spectroscopy **38**, 16 (1971).
13. Kim, J. B., Leonard, J. J., Longo, F. R.: J. Amer. chem. Soc. [in press 1972].
14. a Eisner, U., Linstead, R. P.: J. chem. Soc. (London) **1955**, 3749.
   b Linstead, R. P.: J. chem. Soc. (London) **1952**, 4839.
   c — unpublished spectra some of which are reproduced in Ref. [**10b**].
15. a Schechtman, B. H.: Technical Report No. 5207-2, Solid State Laboratory, Stanford University (1968).
   b —, Spicer, W. E.: J. molecular Spectroscopy **33**, 28 (1969).
16. Hochstrasser, R. M., Marzzacco, C.: J. chem. Physics **49**, 971 (1968).
17. Schaffer, A. M.: Ph. D. thesis, Department of Chemistry, University of Washington, Seattle (1972).
18. a Eastwood, D., Edwards, L., Gouterman, M., Steinfeld, J.: J. molecular Spectroscopy **20**, 381 (1966), Paper VII.
   b Edwards, L., Gouterman, M.: J. molecular Spectroscopy **33**, 292 (1969), Paper XV.
19. Bajema, L., Gouterman, M., Rose, C. B.: J. molecular Spectroscopy **39**, 421 (1971), Paper XXIII.
20. Shashoua, V. E.: J. Amer. chem. Soc. **86**, 2109 (1964); **87**, 4044 (1965).
21. Dratz, E. A.: Ph. D. Thesis, University of California, Berkeley [Radiation Lab. Report UCRL-17200], (1966).
22. a Malley, M., Feher, G., Mauzerall, D.: J. molecular Spectroscopy **26**, 320 (1968).
   b —: Private communication.
23. Pershan, P. S., Gouterman, M., Fulton, R. L.: Molecular Physics **10**, 397 (1966).
24. Chong, D. P.: Molecular Physics **14**, 275 (1968).
25. a Ditchburn, R. W.: Light, p. 469. New York: Interscience (1963).
   b Bernheim, R.: Optical Pumping, p. 6. New York: W. A. Benjamin (1965).
26. Kobayashi, H., Shimizu, M., Fujita, I.: Bull. chem. Soc. Japan **43**, 2335 (1970).
27. a Briat, B., Schooley, D. A., Records, R., Bunnenberg, E., Djerassi, C.: J. Amer. chem. Soc. **89**, 6170 (1967).
   b Djerassi, C.: Private communication.
28. Stephens, P. J., Schatz, P. N., Ritchie, A. B., McCaffery, A. J.: J. chem. Physics **48**, 132 (1968).
29. Sutherland, J. C., Axelrod, D., Klein, M. P.: J. chem. Physics **54**, 2888 (1971).
30. Clementi, E.: J. chem. Physics **40**, 1944 (1964), and IBM Tech. Rept. RJ-256, August, (1963).
31. Silverstone, H. J., Joy, H. W., Orloff, M. K.: J. Amer. chem. Soc. **88**, 1325 (1966).
32. Perrin, M. H., Gouterman, M., Perrin, C. L.: J. chem. Physics **50**, 4137 (1969).
33. Stern, A., Pruckner, F.: Z. Physik. Chem. **178** A, 420 (1937).
34. Longuet-Higgens, H. C., Rector, C. W., Platt, J. R.: J. chem. Physics **18**, 1174 (1950).
35. Zerner, M., Gouterman, M.: Theoret. chim. Acta (Berl.) **4**, 44 (1966), Paper IV.

Dr. A. J. McHugh
130 Jiddens Wharf Rd.
Killara, NSW 2071
Australia

Prof. Dr. Martin Gouterman
Department of Chemistry
University of Washington
Seattle, Washington 98105
USA

Dr. C. Weiss, Jr.
International Bank
for Reconstruction and Development
1818 H Street, N.W.,
Washington, DC 20433, USA